

Live-cell super-resolution imaging with trimethoprim conjugates

Richard Wombacher^{1,5,6}, Meike Heidbreder^{2,6},
Sebastian van de Linde^{3,6}, Michael P Sheetz⁴,
Mike Heilemann², Virginia W Cornish¹ &
Markus Sauer³

The spatiotemporal resolution of subdiffraction fluorescence imaging has been limited by the difficulty of labeling proteins in cells with suitable fluorophores. Here we report a chemical tag that allows proteins to be labeled with an organic fluorophore with high photon flux and fast photoswitching performance in live cells. This label allowed us to image the dynamics of human histone H2B protein in living cells at ~20 nm resolution.

Fluorescence microscopy allows cellular processes to be studied noninvasively with high temporal resolution in three dimensions. But because fluorescence microscopy suffers from diffraction, the spatial resolution had until recently been limited to about 200 nm in the imaging plane, substantially greater than the size of many cellular structures. This constraint has been removed by recent advances in ‘super-resolution’ microscopy that break the diffraction limit through temporal control of the emission of a fluorophore label using either deterministic approaches as in stimulated emission depletion microscopy (STED)¹ and structured illumination microscopy², or stochastic approaches^{3–6} as in photoactivated localization microscopy (PALM)³, fluorescence PALM (FPALM)⁴, stochastic optical reconstruction microscopy (STORM)⁵ and direct STORM (dSTORM)⁶. For the stochastic methods, photoactivatable fluorescent protein labels have the advantage that they allow dynamic measurements in live cells because they are genetically encoded^{3,4,7}. Thus far, organic fluorophores have only been used for super-resolution imaging of proteins in living cells using STED in combination with chemical tags⁸. In addition to having tunable photoswitching rates, reversibly photoswitchable fluorophores can emit orders of magnitude more photons because they survive under moderate excitation conditions for prolonged time periods and can be imaged repeatedly without irreversible photobleaching^{6,9,10}. Therefore, they have the potential to improve the spatial and temporal resolution of stochastic localization methods,

but to date specific labeling of proteins inside cells with reversibly photoswitchable organic fluorophores has been limited to antibody targeting in fixed cells.

Here we report a trimethoprim chemical tag (TMP tag) suitable for stochastic single molecule–based localization microscopy according to the dSTORM method that combines the advantage of genetic encoding with a high photon-output photoswitchable organic fluorophore to enable dynamic live-cell fluorescence imaging with a resolution of ~20 nm^{6,9}. The chemical tags are a surrogate to the fluorescent proteins in which a genetically encoded polypeptide tag is labeled with a modular organic fluorophore¹¹. The TMP tag, which is based on the high-affinity non-covalent (and recently engineered covalent¹²) interaction between *Escherichia coli* dihydrofolate reductase (eDHFR) and trimethoprim, is one of the few chemical tags that can be used to label intracellular proteins in live cells¹³ with high signal-to-noise ratio (Fig. 1a). Because eDHFR has a molecular weight (18 kDa) two-thirds that of GFP and is a stable, monomeric protein, eDHFR is an attractive protein chemical tag^{12,13}. The trimethoprim-fluorophore conjugates have no apparent toxicity, can be synthesized in a few steps (Supplementary Note 1 and Supplementary Figs. 1 and 2) and are readily cell permeant, reflecting the use of trimethoprim clinically as an antibiotic.

For the fluorophore, we used ATTO655, which is an ideal organic fluorophore for super-resolution imaging. It has recently been shown that the reducing environment of the cell catalyzes the reversible photoswitching of ATTO655 (ref. 9); in contrast, many organic fluorophores require deoxygenated environments for efficient photoswitching^{5,6,10}. This photoswitching is an inherent property of ATTO655 and does not require precise conjugation to a second fluorophore⁵. Finally, ATTO655 undergoes photoswitching at timescales that are a function of laser power and compatible with dynamic super-resolution imaging⁹.

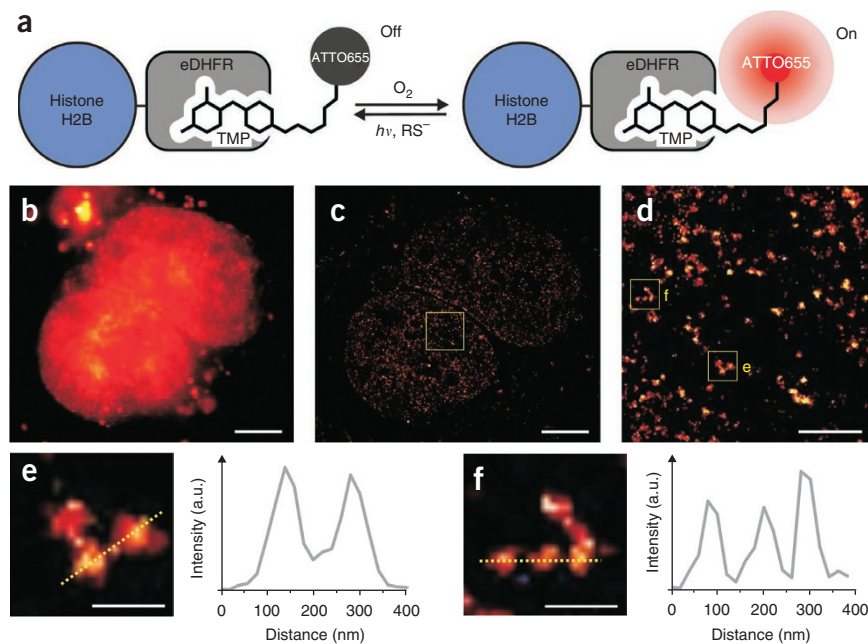
We evaluated the utility of TMP-ATTO655 for dSTORM by labeling human histone H2B protein in live mammalian cells. We transfected HeLa cells with a plasmid encoding histone H2B tagged with eDHFR (H2B-eDHFR), incubated the cells with TMP-ATTO655 for 60 min and imaged them with a confocal laser-scanning fluorescence microscope; we observed specific labeling of histone H2B in the nuclei (Supplementary Fig. 3). When we added TMP-ATTO655 to the culture medium, it rapidly diffused into mammalian cells and labeled the H2B-eDHFR fusion proteins. For dSTORM imaging we used widefield excitation and an inclined illumination scheme to image single molecules in the nucleus of living cells with a high signal-to-noise

¹Department of Chemistry, Columbia University, New York, New York, USA. ²Applied Laser Physics and Laser Spectroscopy, Bielefeld University, Bielefeld, Germany.

³Department of Biotechnology & Biophysics, Julius Maximilians University Wuerzburg, Wuerzburg, Germany. ⁴Department of Biological Sciences, Columbia University, New York, New York, USA. ⁵Present address: Institute of Pharmacy and Molecular Biotechnology, Heidelberg University, Heidelberg, Germany.

⁶These authors contributed equally to this work. Correspondence should be addressed to V.W.C. (vc114@columbia.edu), M.H. (heileman@physik.uni-bielefeld.de) or M.S. (m.sauer@uni-wuerzburg.de).

Figure 1 | dSTORM of core histones using the TMP tag. (a) Schematic representation of the TMP-eDHFR labeling system used for dSTORM. Trimethoprim (TMP), covalently attached to ATTO655, binds H2B-eDHFR. Upon irradiation at 647 nm, ATTO655 is efficiently transferred to a reduced nonfluorescent state ('off') in the presence of millimolar concentrations of glutathione (RS^-). The fluorescent state ('on') is recovered upon reaction with molecular oxygen⁹. This reversible photoswitching enables super-resolution imaging in living cells. (b–f) Live-cell imaging in DMEM medium at room temperature (20 °C). Widefield fluorescence image of TMP-ATTO655-bound core histone H2B proteins in the nucleus of living HeLa cells (b) and corresponding dSTORM image reconstructed from 10,000 images recorded upon excitation at 647 nm with 5 kW cm^{-2} at a frame rate of 50 Hz (~3 min acquisition time) and using an inclined illumination scheme¹⁴ (c). The image in d is an expanded view of the boxed area in c. Expanded views of the marked regions in d (left) and cross-sectional profiles along the dashed lines are shown in e and f. Scale bars, 5 μm (b,c), 1 μm (d), 200 nm (e,f).



ratio¹⁴. We found that by applying an excitation intensity of $0.5\text{--}5 \text{ kW cm}^{-2}$ at 647 nm, ATTO655 fluorophores showed pronounced reversible photoswitching (Supplementary Videos 1–3) under physiological conditions. Our data indicate that these intensities of red laser light applied for 30 min did not cause obvious cell damage. The cells' edges continuously probed their environment and did not show any tendency to retract from the illumination. Typically, we detected 500–1,500 photons from the 'on' state and used this for position determination. This photon output predicts a theoretical precision of single-molecule localization of 5–10 nm¹⁵. Experimentally, a precision of ~20 nm has been achieved with immobilized ATTO655-labeled antibodies⁹.

We reconstructed dSTORM images from 5,000–10,000 images at frame rates of 10–50 Hz corresponding to acquisition times of a few minutes for a total image. Short acquisition times were important to avoid mechanical stabilization or drift correction (Supplementary Fig. 4). Typically, 'off' times of ATTO655 fluorophores in the nucleus varied between a few hundred milliseconds to several tens of seconds, whereas we adjusted 'on' times to 20–100 ms by the excitation intensity depending on the frame rate used (Supplementary Videos 1–3 recorded at different excitation intensities and frame rates). A high ratio of the off to on time and a high stability of the off state are important prerequisites for super-resolution fluorescence imaging of cellular structures in living cells.

dSTORM images had substantially increased resolution over the widefield fluorescence image and allowed the identification of histones incorporated in nucleoprotein complexes in interphase nuclei (Fig. 1b–d). In eukaryotic cells, DNA is organized in nucleosomes with the aid of histones. Two copies of each histone protein, H2A, H2B, H3 and H4, are assembled into an octamer and ~146 base pairs of DNA are wrapped around the octamer to form a nucleosome core. These highly conserved nucleoprotein complexes are usually packed together with histone H1 to form compact fibers 30–40 nm in diameter¹⁶. As histone H2B is subject to slow exchange, we cannot expect complete labeling¹⁷. Nevertheless, the labeling density achieved

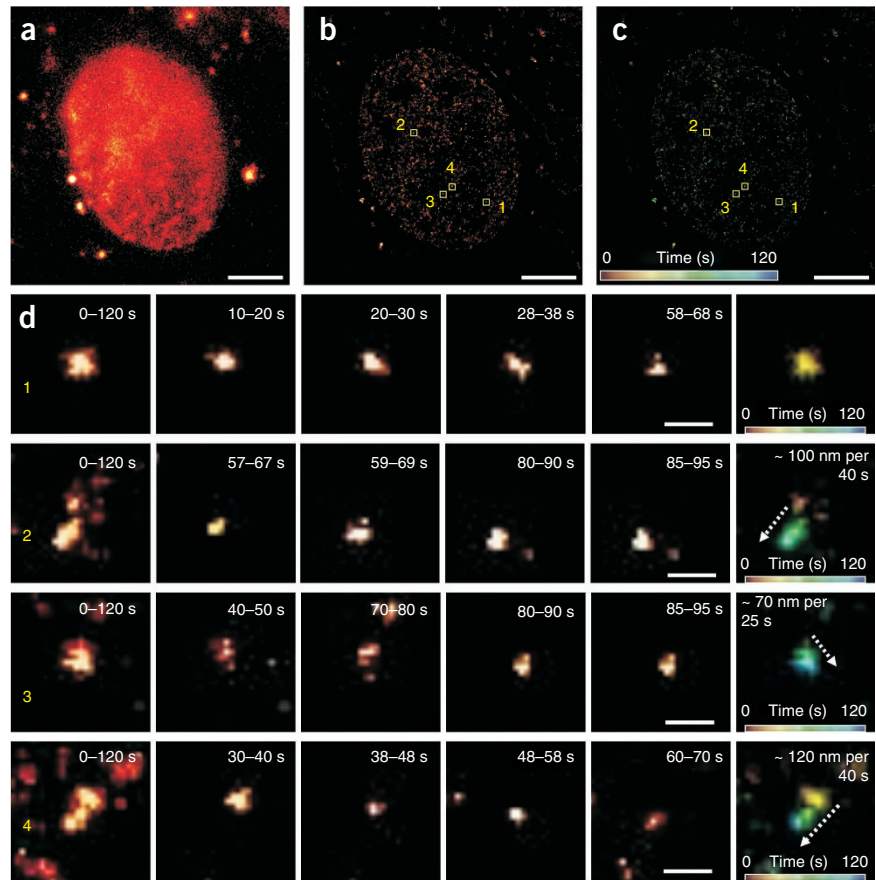
was high enough to unravel structural details hidden in diffraction-limited fluorescence microscopy (Fig. 1b–d).

Analysis of some regions of the nucleus showed that we could resolve distances of ~100 nm between adjacent histone core proteins (Fig. 1e,f). Chromatin is essentially immobile at spatial scales greater than 400 nm but moves inside these restricted 'loci' up to a few hundred nanometers in 10 s, with movement strongly dependent on the cell-cycle phase¹⁸. Therefore, the signals in the dSTORM images appeared blurred with diameters of 30–80 nm (Fig. 1e,f), that is, slightly larger than expected for compact chromatin fibers but well below the resolution limit of confocal microscopy.

To investigate nucleosome and chromatin movement in living cells, we reconstructed super-resolution images from 500 frames (corresponding to a temporal resolution of 10 s at a frame rate of 50 Hz) (Fig. 2 and Supplementary Video 3). Applying a sliding window algorithm we generated highly resolved dSTORM movie sequences from subsets of 500 subsequent frames moving the window always by 50 frames. This allows us to follow dynamics with high spatiotemporal resolution. The applied sliding window procedure did not increase the time resolution of the method but enabled the construction of video sequences from single-molecule localization data (Supplementary Video 4). In dSTORM and PALM, several hundred fluorescence photons are detected per individual fluorophore before they are photo-bleached or photoswitched. Therefore, the localization precision of individual fluorophores achieved in dSTORM and PALM are almost similar^{3–6,9}. However, because reversibly photoswitchable fluorophores can be imaged repeatedly without irreversible photo-bleaching at higher switching rates, orders of magnitude more photons are detected and dynamic processes even of small individual cellular structures can be observed for longer time scales with high frame rates.

We reconstructed images from dSTORM sequences for different core histones (Fig. 2). The sliding window dSTORM method we applied revealed movement of ~3 nm s⁻¹ for interphase nuclei and emphasized

Figure 2 | Dynamic dSTORM imaging of the movement of histone H2B core proteins in the nucleus of living HeLa cells. (a,b) Widefield fluorescence image (a) and corresponding dSTORM image (b). (c) Dynamic dSTORM image reconstructed from 6,000 frames corresponding to a total acquisition time of 120 s. (d) We selected signals of core histone proteins (boxes labeled 1–4 in b and c) to analyze histone mobility in interphase nuclei. Every second (corresponding to 50 frames) a new image was reconstructed and color-coded for time to project the movement. Representative expanded views of signals in regions 1–4 are shown for the indicated time intervals. Signal in region 1 was immobile during the observation time, whereas signals in regions 2–4 moved with a velocity of $\sim 3 \text{ nm s}^{-1}$. Scale bars, 5 μm (a–c) and 200 nm (d).



the importance of the method for dynamic live-cell super-resolution imaging with small tailored organic fluorophores. Owing to fast photoswitching rates, high fluorescence quantum yields and favorably red-shifted absorption and emission properties of fluorophores suited for live-cell imaging, dSTORM is a complementary super-resolution imaging method that can be combined with PALM for multicolor applications.

Our results demonstrate that the dSTORM TMP tag, used for subdiffraction-resolution imaging based on localization of single fluorophores, substantially improves the spatiotemporal resolution possible in live cells. Although chemical tags have recently been reported for use with STED⁸, these STED tags do not exploit photoswitchable organic fluorophores and thus do not improve resolution as does TMP-ATTO655. High excitation intensities of the depletion laser promote photobleaching and limit the observation of dynamic processes in living cells to a few readout frames⁸. The TMP tag is straightforward to implement, and the TMP-ATTO655 dSTORM label can be immediately adopted by non-experts in the chemical tagging field and requires orders of magnitude lower irradiation intensities. Moreover, it should be relatively straightforward to develop orthogonal dSTORM chemical tags for multicolor super-resolution imaging. In combination with photoactivatable fluorescent proteins, such photoswitchable chemical tags should be widely useful for studying the mechanisms of biological processes in living cells.

METHODS

Methods and any associated references are available in the online version of the paper at <http://www.nature.com/naturemethods/>.

Note: Supplementary information is available on the Nature Methods website.

ACKNOWLEDGMENTS

This work was supported by the Biophotonics and the Systems Biology Initiative (Forschungseinheiten der Systembiologie) of the Bundesministerium für Bildung und Forschung and by the US National Institutes of Health (R01GM54469 and RC1GM091804 to V.W.C. and M.P.S.). R.W. was supported by a Deutscher Akademischer Austausch Dienst fellowship.

AUTHOR CONTRIBUTIONS

R.W., M.H., S.v.d.L., M.P.S., M.H., V.W.C. and M.S. conceived and designed the experiments. R.W., M.H. and S.v.d.L. performed the experiments. M.H., S.v.d.L. and M.S. analyzed the data. R.W., V.W.C. and M.S. wrote the paper.

COMPETING FINANCIAL INTERESTS

The authors declare competing financial interests: details accompany the full-text HTML version of the paper at <http://www.nature.com/naturemethods/>.

Published online at <http://www.nature.com/naturemethods/>.

Reprints and permissions information is available online at <http://npg.nature.com/reprintsandpermissions/>.

- Hell, S.W. *Science* **316**, 1153–1158 (2007).
- Kner, P. *et al. Nat. Methods* **6**, 339–342 (2009).
- Betzig, E. *et al. Science* **313**, 1642–1645 (2006).
- Hess, S.T., Girirajan, T.P. & Mason, M.D. *Biophys. J.* **91**, 4258–4272 (2006).
- Rust, M.J., Bates, M. & Zhuang, X. *Nat. Methods* **3**, 793–796 (2006).
- Heilemann, M. *et al. Angew. Chem. Int. Edn.* **47**, 6172–6176 (2008).
- Manley, S. *et al. Nat. Methods* **5**, 155–157 (2008).
- Hein, B. *et al. Biophys. J.* **98**, 158–163 (2010).
- Heilemann, M. *et al. Angew. Chem. Int. Edn.* **48**, 6903–6908 (2009).
- Fölling, J. *et al. Nat. Methods* **5**, 943–945 (2008).
- Miller, L.W. & Cornish, V.W. *Curr. Opin. Chem. Biol.* **9**, 56–61 (2005).
- Gallagher, S.S. *et al. ACS Chem. Biol.* **7**, 547–556 (2009).
- Miller, L.W. *et al. Nat. Methods* **2**, 255–257 (2005).
- Tokunaga, M., Imamoto, N. & Sogawa, S. *Nat. Methods* **5**, 159–161 (2008).
- Thompson, R.E., Larson, D.R. & Webb, W.W. *Biophys. J.* **82**, 2775–2783 (2002).
- Woodcock, C.L. *et al. Proc. Natl. Acad. Sci. USA* **90**, 9021–9025 (1993).
- Kimura, H. & Cook, P.R.J. *Cell Biol.* **153**, 1341–1353 (2001).
- Heun, P. *et al. Science* **294**, 2181–2186 (2001).

ONLINE METHODS

General methods. Unless otherwise noted, reagents were obtained from Aldrich and used without further purification. Nuclear magnetic resonance (NMR) spectra were recorded on a Bruker 400 (400 MHz) Fourier transform NMR spectrometer at the Columbia University Department of Chemistry NMR facility. Spectra were taken in deuterated methanol, using the solvent residual peaks as reference. Fast atom bombardment (FAB) Mass spectra were recorded at the Columbia University Department of Chemistry Mass on a JMS-HX110A mass spectrometer. Absorption spectra were recorded on a Spectramax Plus384 UV-visible spectrophotometer (Molecular Devices). Preparative HPLC was performed on a Waters 600 using a C18 column. Compound 1 (**Supplementary Fig. 1**) was synthesized from trimethoprim according to a previously published report¹⁹ (**Supplementary Note 1**). Purified dry TMP-ATTO655 was dissolved in DMF to a 2.5 mM concentration as a stock solution for cell labeling experiments. The concentration was determined based on the UV-light absorbance at 663 nm in diluted aqueous solution according to the extinction coefficient for ATTO655 (maximum wavelength (λ_{max}) = 663 nm, maximum extinction coefficient (ϵ_{max}) = $1.25 \times 10^5 \text{ M}^{-1} \text{ cm}^{-1}$). TMP-ATTO655 was characterized by NMR spectroscopy (**Supplementary Fig. 2**).

Plasmid vector construction. *H2B-eDHFR* was generated by replacing *EGFP* in *H2B-EGFP* (Addgene plasmid 11680) by *eDHFR*³. *H2B-EGFP* plasmid was digested with the restriction enzymes AgeI and NotI. The gene encoding eDHFR was generated from plasmid pLL-1-NFkB-p65 (Active Motif, Inc.) using the primers 5'-ACGTCACCGGTGCGCCACCATGGTGGGTTCTGGTGGTTCTGGTATCAGTCTGATTGCGGCG-3' (AgeI) and 5'-ACGTCGCGGCCGCTTTAGTGATGGTGGTGGTATGCCGCCGCTCCAGAATCT-3' (NotI) and inserted into the digested vector to generate the *H2B-eDHFR* plasmid.

Cell culture and labeling. HeLa cells were grown at 37 °C and 5% CO₂ in high-glucose DMEM (Gibco) supplemented with 10% FCS (Gibco) and split every other day. Approximately 2×10^6 cells were transfected by electroporation, using the Amaxa Nucleofector System according to the manufacturer's instructions (Lonza). Transfected cells were allowed to grow in 8-well Labtek chambers (Nunc) overnight. Cells were stained using $2.5 \times 10^{-8} \text{ M}$ TMP-ATTO655 for 1 h at 37 °C by adding the conjugate directly to the growth medium. To decrease unspecific membrane stain, cells were washed with PBS (pH 7.4) and incubated for another hour in fresh DMEM. Cells were detached from the glass surface using PBS and trypsin (0.25%) at 37 °C and transferred into a new Labtek chamber that was cleaned with 1% aqueous hydrogen fluoride for 10 s and washed with PBS. Cells were allowed to reattach to the glass surface for 1–3 h before imaging. Imaging was done in standard DMEM at room temperature (20 °C). The cells did not show apparent ill defects after imaging and were incubated again at 37 °C and 5% CO₂ in DMEM overnight to verify normal growth and cell division.

To test specific labeling of histone H2B in the nucleus of living cells we performed staining experiments with the intercalating fluorophore Sytox blue (Invitrogen) and confocal laser scanning fluorescence images on a LSM710 (Carl Zeiss Micro Imaging). We observed nuclear localization of TMP-ATTO655 and a transfection efficiency of 40–50% (**Supplementary Fig. 3**).

Nontransfected but equally labeled cells showed no fluorescence signals demonstrating specific labeling of histone H2B. Unspecific labeling of cells and adsorption of TMP-ATTO655 on glass surfaces was only rarely observed (**Supplementary Fig. 3**).

dSTORM imaging. Super-resolution fluorescence imaging was performed on an inverted microscope (Olympus IX-71) equipped with an oil-immersion objective (60 \times , numerical aperture (NA) 1.45; Olympus)^{6,9,20}. The 647 nm laser line from an argon krypton laser (Coherent) was selected by an acousto-optic tunable filter (AAOptics), reflected by a dichroic beamsplitter (FF560/659; Semrock) and focused onto the back focal plane of the microscope objective. An inclined illumination scheme was used to image single molecules in nuclei of living cells with high signal-to-noise ratio¹⁴. The fluorescence light was collected by the same objective, filtered by a bandpass filter (ET700/75; AHF Analysentechnik) and a longpass filter (HQ665LP, AHF Analysentechnik) and imaged on an electron-multiplying charge-coupled device (CCD) camera (Ixon DV897; Andor). Additional lenses were used to achieve a final imaging magnification of 160 times on the CCD chip corresponding to a pixel size of 100 nm. We measured 5,000–10,000 frames with a frame rate of 10 to 50 Hz, applying irradiation intensities of 0.5 to 5 kW cm⁻². For a typical measurement time of a few minutes (1–5 min) we did not observe a detectable drift. That is, we achieved a localization accuracy of better than 20 nm, implying negligible drift. To validate this observation we performed experiments with quantum dots adsorbed on a coverslip (**Supplementary Fig. 4**). In all experiments we found individual immobile structures or fluorophores (for example, inside of the nucleus (**Fig. 2**) or adsorbed to the glass surface next to a cell) as reference points to follow any drift in the image stack.

Data analysis. Fluorescence images were analyzed to reconstruct super-resolved images using rapid-dSTORM software as described previously²¹. Fluorescence signals containing less than 500 or more than 2,000 photons were discarded. Highly resolved video sequences were generated using stacks of 500 inclined illumination images to reconstruct dSTORM images. Then, a sliding window algorithm was applied to generate a new dSTORM image every 50 images²². The sliding window analysis was used to smooth the transitions between subsequent images of a movie. When rendering the frames independently (that is, frames 1–500, 501–1,000, 1,001–1,500 and so on), identical movement was observed but the transitions between subsequent images appeared very rugged.

The effect of photoswitching kinetics and labeling densities. The ability to resolve a structural feature (that is, the achievable experimental resolution) is controlled by the brightness of the fluorophores used, the labeling density and the stability or lifetime of the off state^{23–25}. Therefore, the ratio of off and on switching of a fluorophore affects the achievable resolution. If the structure to be imaged is labeled with a high fluorophore density, the lifetime of the off state, τ_{off} should be substantially longer than the lifetime of the on state, τ_{on} . The highest localization precision is achieved for very short τ_{on} accompanied by a high fluorescence quantum yield^{23,24}. Upon irradiation the fluorophore is transferred to a metastable off state at a rate k_{off} where it resides until it is converted to the singlet ground state with rate k_{on} . We define the ratio

of these rates as $r = k_{\text{off}}/k_{\text{on}} = \tau_{\text{off}}/\tau_{\text{on}}$.²³ For relatively unstable off states with short τ_{off} , high irradiation intensities have to be applied to reduce τ_{on} and to generate a sufficient r , for example, $r = 100$ for $\tau_{\text{on}} = 1$ ms and $\tau_{\text{off}} = 100$ ms. In the case of off-state lifetimes in the range of seconds, a sufficient high rate r can be achieved with comparably long on times (and corresponding low irradiation intensity). In addition, r can be optimized applying higher irradiation intensities. Thus, τ_{on} decreases and enables higher imaging speed. This has the additional advantage that other effects such as mechanical drifts are reduced and becomes in particular important when dynamic processes are observed. The more densely a structure is labeled with photoswitchable fluorophores, the higher the ratio r has to be to ensure that fluorescence emission of single fluorophores is temporally well separated to allow unambiguous localization of individual emitters. A ratio $r = 200$ –1,000 measured for ATTO655 under physiological conditions enables dense

labeling as a prerequisite for dSTORM with high optical resolution²⁶. In principle, the ratio can be easily increased by applying higher excitation intensities. However, higher irradiation intensities can cause cell damage and therefore have to be avoided in live-cell imaging. This highlights the importance of very stable off states with lifetimes of several seconds for super-resolution imaging under physiological conditions.

19. Calloway, N.T. *et al. ChemBioChem* **8**, 767–774 (2007).
20. van de Linde, S. *et al. Photochem. Photobiol. Sci.* **8**, 465–469 (2009).
21. Wolter, S. *et al. J. Microsc.* **237**, 12–22 (2010).
22. Endesfelder, U. *et al. ChemPhysChem* **11**, 836–840 (2010).
23. van de Linde, S., Wolter, S., Heilemann, M. & Sauer, M. *J. Biotechnol.* advance online publication 20 February 2010 (doi:10.1016/j.jbiotec.2010.02.010).
24. Cordes, T. *et al. Nano Lett.* **10**, 645–651 (2010).
25. Shroff, H., Galbraith, C.G., Galbraith, J.A. & Betzig, E. *Nat. Methods* **5**, 417–423 (2008).
26. Shannon, C.E. *Proceedings of the Institute of Radio Engineers* **37**, 10–21 (1949).